Int. J. Heat Mass Transfer. Vol. 7, pp. 1419–1425. Pergamon Press 1964. Printed in Great Britain

EFFECT OF GAS ENTRAINMENT ON LIQUID METAL HEAT TRANSFER

TOKURO MIZUSHINA, TADAHISA SASANO*, MINORU HIRAYAMA†, NAOKI OTSUKI‡ and MASAAKI TAKEUCHI§

Department of Chemical Engineering, Kyoto University, Kyoto, Japan

(*Received* 15 *May* 1964)

Abstract—Nitrogen and helium gases were mixed quantitatively into the turbulent flow of mercury in a horizontal and a vertical tube heat exchanger, and the effect on decreasing the heat-transfer coefficient was observed.

NOMENCLATURE

A_i, inside heat-transfer surface area [m²];

A_o, outside heat-transfer surface area [m²];

C_p, specific heat of mercury [kcal/kg degC];

D, inside diameter of tube [m];

h_{Hg}, heat-transfer coefficient of mercury flow [kcal/m² h degC];

h_{ov}, overall heat-transfer coefficient based on inside surface area consisted of all thermal conductances other than mercury film coefficient [kcal/m² h degC];

k_{Hg}, thermal conductivity of mercury [kcal/m h degC];

l, length of capillary [m];

p, pressure of gas [kg/cm² gauge];

Q, heat-transfer rate [kcal/h];

q_o, heat flux at outside surface [kcal/m² h];

r, radius of capillary [m];

t, temperature [°C];

$(\Delta t)_{lm}$, logarithmic mean temperature difference [degC];

U, overall coefficient of heat transfer [kcal/m² h degC];

V_{Hg}, flow rate of mercury [m³/h];

V_g, flow rate of gas [m³/h];

α, ratio of area covered by gas bubbles to total tube wall surface;

μ, viscosity of gas [kg/m h];

ρ, density of mercury [kg/m³];

Nu, Nusselt number;

Nu_{av}, Nusselt number averaged for total length of tube;

Pe, Peclet number.

INTRODUCTION

SOME OF THE investigators who studied on liquid-metal heat transfer in circular tubes obtained values of the heat-transfer coefficients much lower than predicted from the Martinelli–Lyon's theoretical equation. There are several possible reasons for this disagreement, but the gas entrainment in the liquid-metal flow may be the most important. Since MacDonald and Quittenton [1] published their paper on the effect of the gas entrainment, many investigators studied on this subject. However, none of them measured the gas–liquid ratio quantitatively and observed its effect on the decrease of heat-transfer coefficient.

In this paper the authors will describe the results of their experiments on the effect of the gas entrainment in the turbulent flow of mercury in vertical and horizontal circular tubes on lowering the heat-transfer coefficient. Nitrogen and helium gases, the thermal conductivity of which are far different from each other, were mixed into the mercury flow through a flow controlling device and gas rate measuring flowmeter.

Present addresses:
* Teijn Co. Ltd.
† Toyo Koatsu Co. Ltd.
‡ Fuji Iron & Steel Co. Ltd.
§ Osaka Gas Co. Ltd.

EXPERIMENTAL APPARATUS AND PROCEDURE

The flow diagram of the apparatus for heat transfer in a horizontal tube is shown in Fig. 1. The mercury is pumped up from the reservoir to the head tank through a cooler with a vertical centrifugal pump of 5 h.p., and flows down

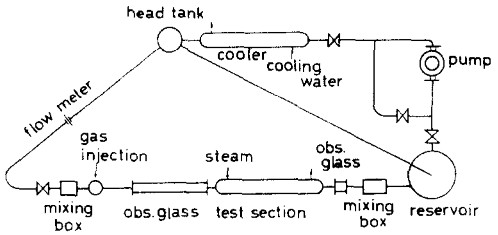

FIG. 1. Experimental apparatus.

through a nozzle flowmeter into the test section which is heated by steam and then returns to the reservoir. The gas entrained was removed from the liquid flow carefully at the outlet mixing box, the reservoir and the head tank. In addition, the vertical part of the liquid circulating pipe before the inlet mixing box was carefully designed and provided with a vent to remove the gas entrained, so as to make the liquid flowing into the inlet mixing box free from gas bubbles.

On the other hand, the gas is mixed into the liquid metal flow through a capillary tube at the inlet mixing box after its flow rate is controlled and measured.

The pipe line is made of the 18–8 stainless steel "SUS27", and the vessels are coated with the resin "Eternal".

The glass tubes are positioned before and after the test section for observing the behaviour of gas bubbles in liquid metal flow.

The detail of test section is shown in Fig. 2. The heat exchanger is made of a "SUS27" stainless steel tube of 30 mm O.D., 26 mm I.D. and 1950 mm in length, and provided with a steam jacket for heating. The temperatures of the mercury flow were measured at the inlet and outlet mixing boxes with mercury thermometers of $\frac{1}{10}$ °C scale, and those of the steam were measured at both ends of the jacket with the copper–constantan thermocouples. The steam jacket is provided with a drain tube for condensate and a vent for uncondensed steam and non-condensable gas. The test section was carefully installed as horizontally as possible using a level gauge.

The flow sheet for the vertical tube heat exchanger is about the same as that for the horizontal one described above. The detail of the vertical tube test section is shown in Fig. 3. The heat exchanger is made of a "SUS27" stainless steel tube of 18 mm O.D., 14 mm I.D. and 1000 mm in length. The steam jacket is divided into four sections, namely 245 mm, 250 mm, 255 mm and 250 mm in length respectively from the bottom. The condensate of steam of the four parts were collected and measured separately. The temperature measurement is as same as for the horizontal test tube. The test section was carefully put as vertically as possible.

The device to control and to measure the gas rate is shown in Fig. 4. The gas tank is large enough to buffer the fluctuation of the gas input from the gas cylinder, and its pressure was kept at 2 kg/cm^2 gauge for the horizontal exchanger and 4 kg/cm^2 gauge for the vertical one. The gas rate was measured with the capillary tube flow meter, using the following equation.

$$pV_g = \frac{\pi r^4}{16\mu l}(p_1^2 - p_2^2) \qquad (1)$$

where V_g is gas volume rate at the pressure p,

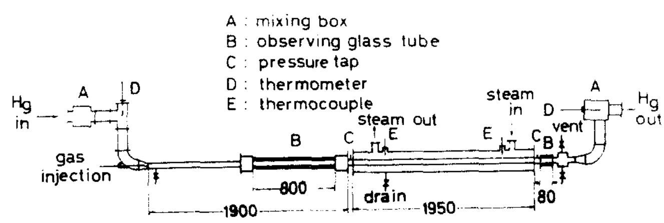

FIG. 2. Horizontal heat exchanger.

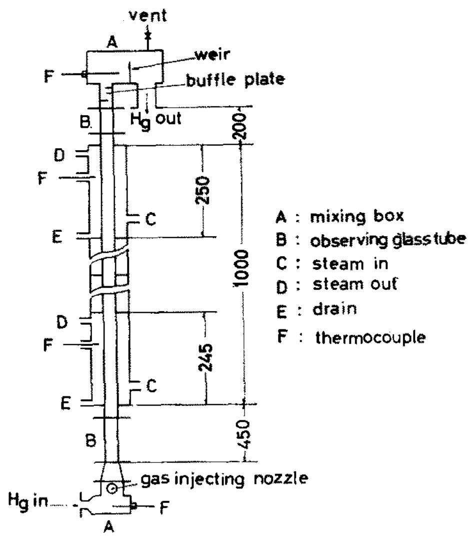

FIG. 3. Vertical heat exchanger.

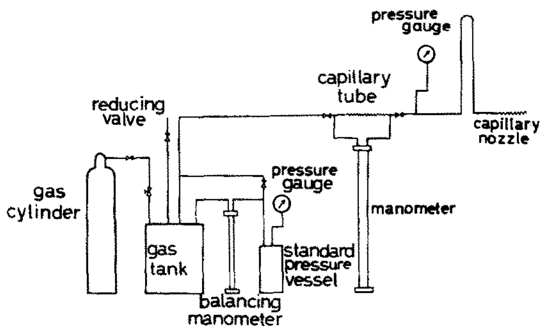

FIG. 4. Controlling and measuring device for gas.

r and l are radius and length of the capillary respectively, μ is viscosity of gas and p_1 and p_2 are pressure before and after the capillary respectively. The velocity fluctuation of the mercury flow sometimes causes a change of the static pressure at the gas inlet, which results in a reverse flow of mercury into the gas injecting capillary tube. In order to prevent this, the capillary tube is designed so as to cause the pressure drop of 3 — 5 mmHg.

The pressure of the heating steam was controlled to be about atmospheric pressure and the steam flow rate was kept much higher than the rate of condensation. The uncondensed steam was forced out from the vent with non-condensable gas.

After the flows of mercury, gas and steam were settled, 2 h were necessary to reach the steady state, and then the measurements were done for three times with 10 min intervals. The flow rates of mercury and gas, the temperatures of mercury flow at inlet and outlet mixing box, heating steam, cooling water and room, and the rate of condensing steam of each heating section were measured and recorded.

In each run the behaviour of gas bubbles in liquid metal flow was observed from the observing glass tubes.

The experimental range of flow rates of mercury and gas for the horizontal and vertical test exchangers are shown in Table 1.

As the preliminary experiments, the following two were executed. (1) In order to determine the heat-transfer coefficient of the condensing steam, heat-transfer experiments with water flow in place of mercury were done. (2) The behaviour of gas bubbles in mercury flow in a horizontal tube was observed with an acryl resin tube of 1 in diameter which replaced the test tube. The eye, 35 mm camera and 8 mm ciné camera were used for observation. The experimental range of the flow rates of mercury and gas was slightly different from those in Table 1. In addition, the same experiment was planned for vertical tube, but the behaviour of the gas bubbles in mercury flow in vertical tubes was found to be completely different from that in the horizontal tubes with the gas being dispersed in the liquid; under these circumstances the gas could not be seen from the outside of the flow.

RESULTS

(1) *Observation of gas bubbles in mercury flow in the horizontal tube*

The flow patterns changed slightly from the inlet to the outlet, but can be classified into three kinds, namely bubble flow, plug flow and stratified flow. The observed results at the inlet observing glass are plotted on a mercury flow rate vs. gas flow rate diagram in Fig. 5, which is similar to the diagram obtained by Alves [2] for water–air and oil–air mixtures. The typical photographic pictures of these three flow patterns are shown in Fig. 6(*a*) (*b*) (*c*).

From the still and ciné pictures of the bubble flow, the ratio of the area which is covered by

Table 1. The experimental range of gas injection rate
[cm^3 at the gas injection nozzle/s]

Horizontal tube Flow rate of mercury (cm^3/s)		600	400	200	150
Re		282 000	188 000	94 000	70 500
	0	0	0	0	0
Gas/liquid ratio	1/5000	0·12	—	—	—
(cm^3/cm^3)	1/2000	0·3	0·2	0·1	—
	1/1000	0·6	0·4	0·2	0·15
	1/500	1·2	0·8	0·4	0·3
	1/200	—	2·0	1·0	0·75
	1/100	—	—	2·0	1·5

Vertical tube Flow rate of mercury (cm^3/s)		120	70	30
Re		105 000	61 200	26 200
	0	0	0	0
Gas/liquid ratio	1/500	0·24	0·14	—
(cm^3/cm^3)	1/200	0·6	0·35	0·15
	1/100	1·2	0·7	0·3
	1/50	2·4	1·4	0·6
	1/20	—	—	1·5

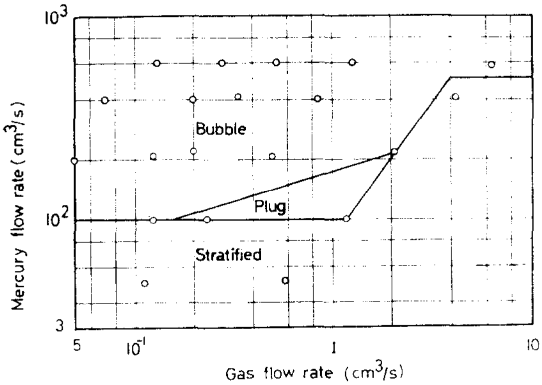

FIG. 5. Flow pattern diagram.

gas bubbles to the total tube wall surface and the velocity of the gas bubble moving along the tube wall were obtained, and the results are plotted in Fig. 7 and 8 respectively.

(2) Heat-transfer coefficient

From the preliminary runs with the turbulent flow of water in the tubes, the following experimental equations for the overall heat-transfer coefficient h_{ov} based on the inside surface area and consisting of all thermal conductances other than the liquid-mercury film coefficient were obtained.

For the horizontal test tube

$$\frac{10^4}{h_{ov}} = 1{\cdot}414 + 1{\cdot}730 \times 10^{-2} q_o^{1/3} \tag{2}$$

For the vertical test tube

$$\frac{10^4}{h_{ov}} = 1{\cdot}460 + 1{\cdot}625 \times 10^{-2} q_o^{1/3} \tag{3}$$

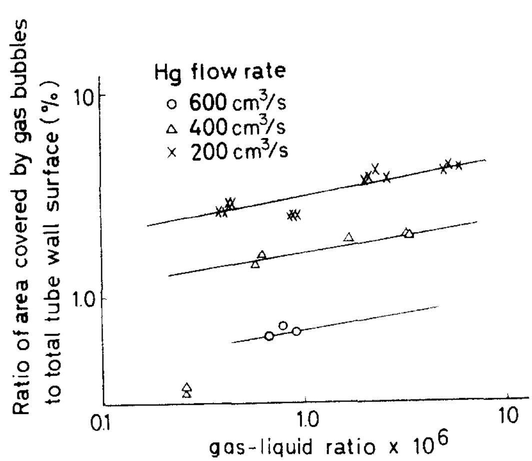

FIG. 7. Area covered by gas bubbles in horizontal tube.

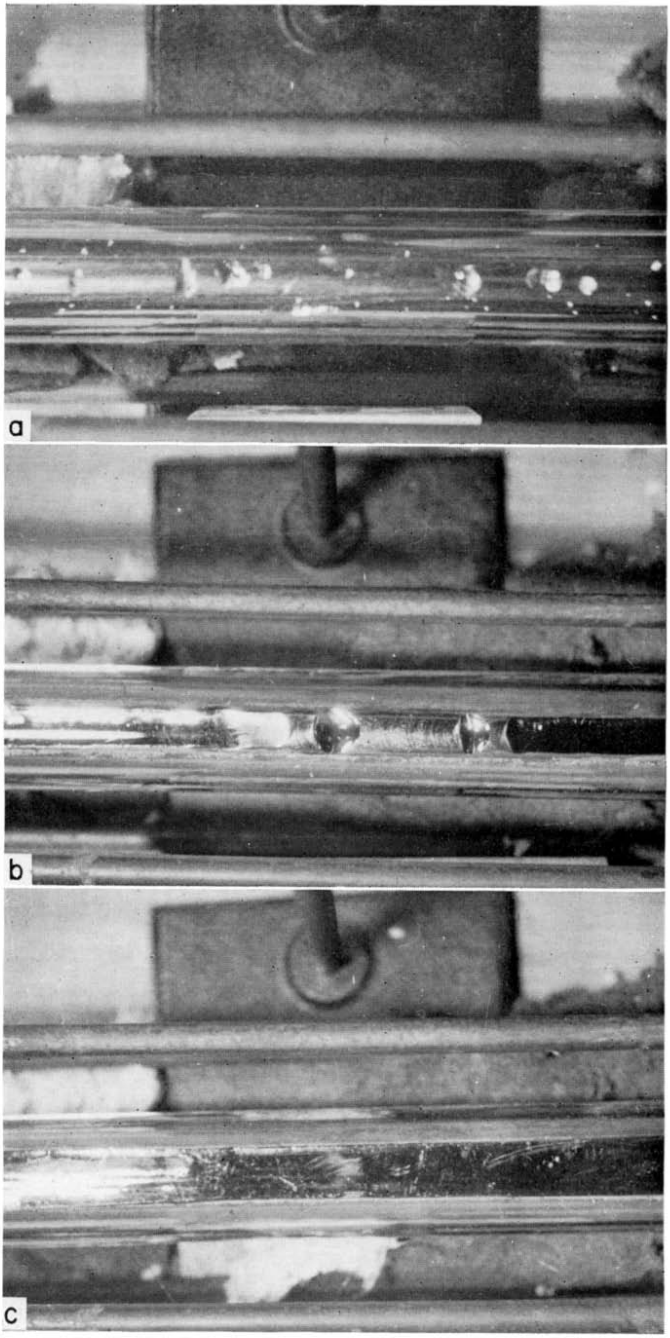

FIG. 6. (*a*) Bubble flow; (*b*) Plug flow; (*c*) Stratified flow.

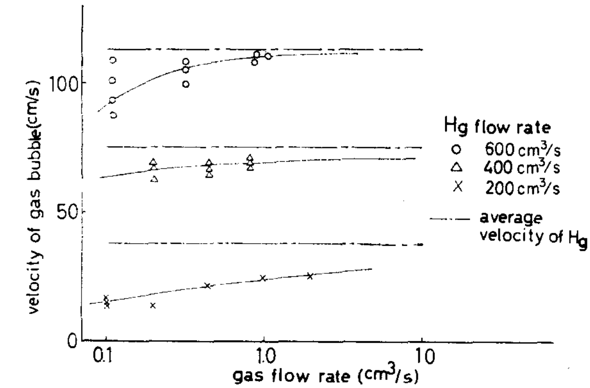

FIG. 8. Velocity of gas bubbles in horizontal tube.

where $q_o = Q/A_o$ is heat flux at outside surface.

On the other hand, the overall coefficient of heat transfer based on the inside surface area was calculated from the following equation:

$$\frac{1}{U} = \frac{Q}{A_i(\Delta t)_{lm}} \tag{4}$$

where A_i is the inside surface area, and $(\Delta t)_{lm}$ is the logarithmic mean temperature difference. The heat-transfer rate Q is calculated from

$$Q = C_p \, \rho \, V_{Hg} (t_2 - t_1) \tag{5}$$

where, C_p, ρ and V_{Hg} is the specific heat, density and flow rate of mercury respectively, and t_1 and t_2 are its temperature at inlet and outlet. The heat-transfer rate was also calculated from the rate of steam condensation, but this value was used only for checking the heat balance.

Then, the heat-transfer coefficient of mercury film was obtained as

$$\frac{1}{(h_{Hg})} = \frac{1}{U} - \frac{1}{h_{ov}} \tag{6}$$

In the case of the vertical test tube, not only total average value of h_{Hg} but the local average value for each separate section was obtained. In this case the value of Q calculated by equation (5) was divided into four by multiplying the ratios of the rate of condensation in each section to the total condensate rate.

Nu_{av} vs. Pe are plotted for the horizontal test tube in Fig. 9, and for the vertical test tube in Fig. 10. For comparison, the theoretical curve is drawn in these diagrams. As described above, the outside of the tube was heated with steam, therefore the temperature of the outside interface was constant. For this case Hirayama [3] corrected Lyon's equation as follows

$$Nu = 5 + 0{\cdot}025 Pe^{0{\cdot}8} + \frac{12 + 0{\cdot}05 Pe^{0{\cdot}8}}{\dfrac{h_{ov}D}{k_{Hg}} + 6 + 0{\cdot}025 Pe^{0{\cdot}8}} \tag{7}$$

This equation, however, gives the heat-transfer coefficient in the fully developed turbulent region. Therefore, the correction factor of Deissler [4]

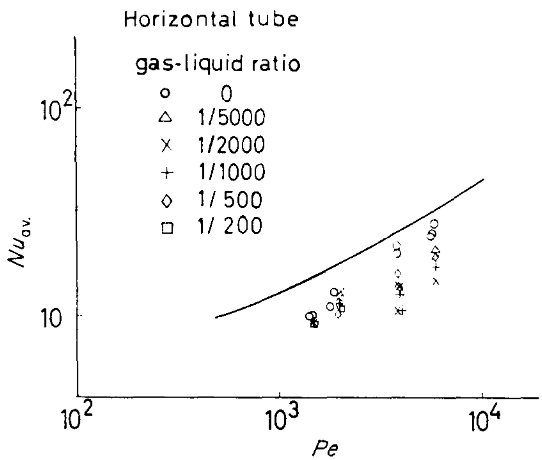

FIG. 9. Experimental results of heat transfer in horizontal tube.

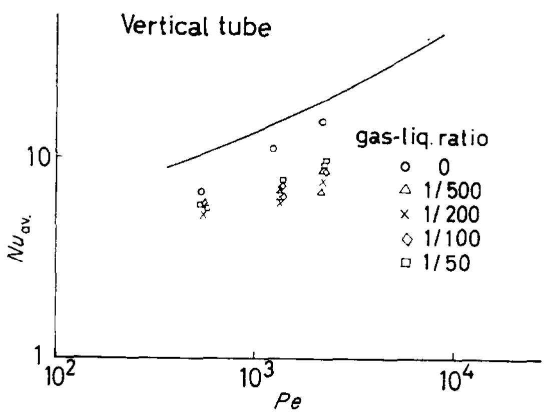

FIG. 10. Experimental results of heat transfer in vertical tube.

is multiplied to the values from equation (7) to obtain the average value of the coefficient. Thus, the theoretical curves in Fig. 9 and 10 are drawn. It is shown that even the heat-transfer coefficients of no gas entrainment are lower than the theoretical values. This disagreement may be attributed to other reasons, for example non-wettingness [5] and the fact that the eddy diffusivity of heat is lower than that of momentum [6].

Nu_{av} is plotted against gas–liquid ratio for the horizontal test tube in Fig. 11, and for the vertical one in Fig. 12. In the case of the horizontal tube, the heat-transfer coefficient decreases sharply with a small amount of entrained gas but becomes almost constant above a certain value of the gas–liquid ratio. At the lower rate of liquid flow the entrained gas does not affect the heat-transfer coefficient at all. The gas entrainment may have two opposite effects on heat transfer, namely a negative effect of mixing the material of low thermal conductivity into liquid flow and a positive effect of increasing the velocity of flow and disturbing the flowing liquid. At the smaller gas–liquid ratio, the former effect overcomes the latter and then, at the higher ratio, these two effects may compensate each other.

In the case of the vertical tube, the result is slightly different from that of the horizontal tube. At first, the transfer coefficient decreases with increasing gas–liquid ratio, but it slowly increases again above a certain value of the ratio. In this region, the positive effect of increased flow velocity may overcome the negative influence of the effective decrease in conductivity.

In Fig. 13 the local average values of heat-transfer coefficient for four sections of the vertical test tube are plotted against the gas–liquid ratio. The tendency is almost the same for each section, but the coefficient at the upper section is smaller than that at lower section. This may be the result of the gas volume change because of the static pressure.

All these figures show that there is no difference between helium and nitrogen though the thermal conductivity of helium is nine times as large as that of nitrogen. This result is the same as Johnson *et al.* [7].

Finally, the decreasing ratio of Nusselt number vs. the ratio of the area which is covered by gas bubbles to the total tube wall surface of

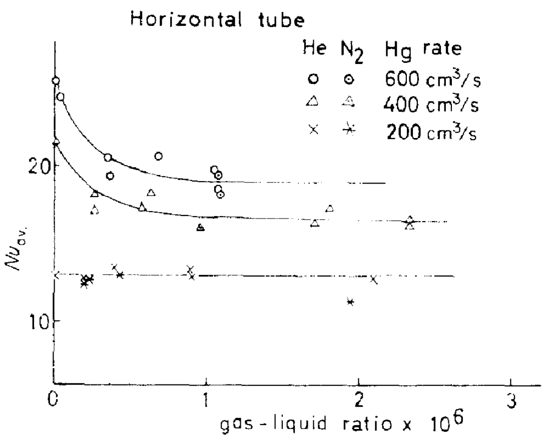

FIG. 11. Effect of gas entrainment in horizontal tube.

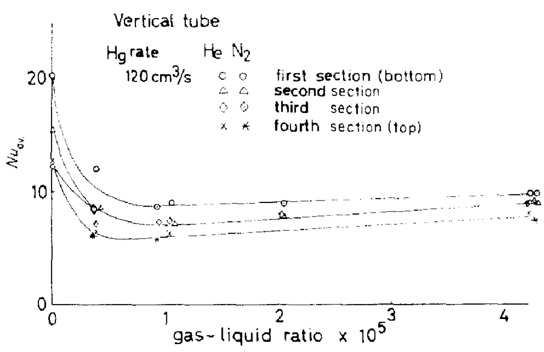

FIG. 12. Effect of gas entrainment in vertical tube.

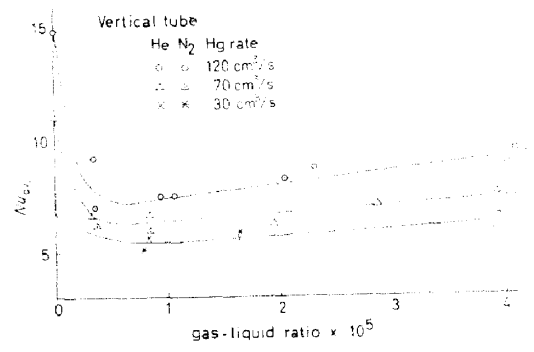

FIG. 13. Local average values of heat-transfer coefficients for four sections of vertical tube.

the horizontal tube are plotted in Fig. 14. The former is much larger than the latter, perhaps because not only the gas bubble on the wall surface but also in the liquid flow interferes with heat flux.

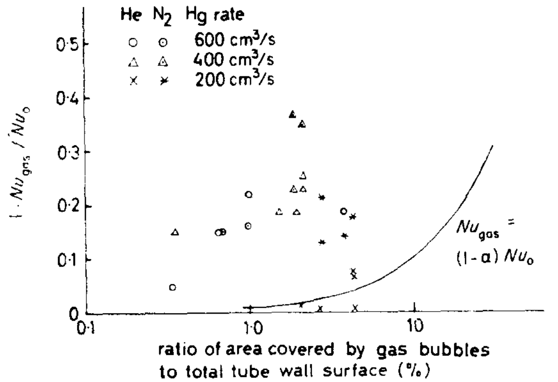

FIG. 14. Relation between decrease of Nusselt number and area covered by gas bubbles in horizontal tube.

CONCLUSIONS

1. The behaviour of entrained gas in liquid metal flow in a horizontal tube and a vertical tube are different each from other. 2. In both cases, a small amount of gas decreases the heat-transfer coefficient remarkably, but the coefficient becomes almost constant above a certain value of the gas–liquid ratio in the horizontal tube and it slowly increases again above a certain value of the ratio in the vertical tube. 3. Even the heat-transfer coefficients of no gas entrainment are lower than the theoretical values. 4. There is no difference between helium and nitrogen for the decreasing effect of the heat-transfer coefficient. 5. There is no proportional relation between the tube wall surface area which is covered by gas bubbles and the decreasing ratio of heat-transfer coefficient of the horizontal tube exchanger.

ACKNOWLEDGEMENTS

The authors wish to express their thanks to the Ministry of Education of Japan, and Asahi Glass Co. Ltd. for their financial support.

REFERENCES

1. W. C. MacDonald and R. C. Quittenton, A critical analysis of metal "wetting" and gas entrainment in heat transfer to molten metals, *Chem. Engng Progr.* Symposium Series, No. 9, **50**, 59–67 (1954).
2. G. E. Alves, Cocurrent liquid-gas flow in a pipe-line contactor, *Chem. Engng Progr.* **50**, 449–456 (1954).
3. M. Hirayama, Heat transfer to liquid metals, Master Thesis at Department of Chemical Engineering of Kyoto University (1962).
4. R. G. Deissler, Analysis of turbulent heat transfer and flow in entrance region of smooth passages, *NACA TN* 3016 (1953).
5. T. Mizushina, S. Iuchi, T. Sasano and H. Tamura, Thermal contact resistance between mercury and a metal surface, *Int. J. Heat Mass Transfer* **1**, 139–146 (1960).
6. T. Mizushina and T. Sasano, The ratio of the eddy diffusivities for heat and momentum and its effect on liquid metal heat-transfer coefficients, *Int. Develop. Heat Transfer* 662–668 and *D*-217-221 (1961).
7. H. A. Johnson, W. J. Clabaugh and J. P. Hartnett, Heat transfer to mercury in turbulent pipe flow, *Trans. Amer. Soc. Mech. Engrs* **76**, 505–511 (1954).

Résumé—De l'azote et de l'hélium ont été mélangés quantitativement dans un écoulement turbulent de mercure, dans un échangeur de chaleur avec des tubes horizontaux ou avec des tubes verticaux, et l'effet sur la décroissance du coefficient de transport de chaleur a été observé.

Zusammenfassung—Stickstoff und Helium wurden in bestimmten Mengen als Gase mit Quecksilber vermischt, das turbulent durch einen waagerechten und senkrechten Rohr-Wärmetauscher strömte. Die Auswirkungen beim Verringern des Wärmeübergangszahl wurde beobachtet.

Аннотация—В турбулентный поток ртути в горизонтальном и вертикальном теплообменнике вдувались газы: азот и гелий, и наблюдалось влияние этого вдува на снижение коэффициента теплоотдачи.